Evaluation of the Shape Memory Behavior of a Poly(cyclooctene)-Based Nanocomposite Device

A. Dorigato, A. Pegoretti
Department of Industrial Engineering and INSTM Research Unit, University of Trento, Trento 38123, Italy

The objective of the present work is to investigate the electro-activated shape memory behavior of a polycyclooctene (PCO) based nanocomposite device. At this aim, carbon black (CB) and exfoliated graphite nanoplatelets (xGnP) were melt compounded with a PCO matrix crosslinked with a dicumylperoxide content of 2 wt% and a total filler amount of 4 wt%. Electrical resistivity measurements on bulk materials evidenced a noticeable decrease of the electrical resistivity upon CB addition, while no synergistic effects were detected mixing CB and xGnP. Nanocomposite with a CB amount of 4 wt% revealed also a noticeable heating capability through Joule effect for voltage levels higher than 100 V. The subsequent characterization of an electro active shape memory device based on this composition demonstrated how it is possible to prepare a shape memory nanocomposite material able to completely recover its original shape after 100 s with a voltage of 90 V. The retention of the shape memory behavior after several (50) programming cycles was also demonstrated. POLYM. ENG. SCI., 58:430–437, 2018.

INTRODUCTION

It is well known that the addition of metal and carbon based nanofillers, such as metal nanopowders, graphite nanoplatelets (GnPs), carbon black (CB), and carbon nanofibers (NFs) could significantly alter the macroscopic properties of polymeric matrices, offering thus new opportunities for the production of innovative multifunctional materials. In particular, the addition of conductive nanofillers could dramatically decrease the electrical resistivity of polymer matrices [1–3]. Above a critical filler loading (i.e., the percolation threshold), conductive nanofillers form a continuous network through the polymer matrix, and the resistivity could be thus dramatically decreased [4]. As an example, the thermomechanical properties and the electrical monitoring capability of a nanomodified epoxy system was recently investigated by our group [5, 6].

The introduction of conductive nanofillers within polymer matrices can be also applied for the development of electroactive shape memory polymers (SMP). SMPs are able to "remember" their original shape to which they return if subjected to a physical stimulus (heat, light, electric, and magnetic fields) [7, 8]. Moreover, novel electrically conducting SMPs filled with carbon nanotubes [9, 10], CB [11], conductive fiber [12], and nickel zinc ferrite ferromagnetic particles, etc. [13] were recently developed to satisfy the technological request of avoiding external heaters. Consequently, several examples of electroactivated composites can be found in literature [14–17], and it was demonstrated how the addition of electrically conductive and/or magnetic nanoparticles in a polymer matrix leads to an effective shape recovery upon an electric or magnetic field application [18].

Some attention was devoted in the past to polycyclooctene (PCO) as SMP matrix [19]. PCO is a polyolefin constituted by an hydrocarbon backbone containing unsaturations. It can be synthesized starting from cyclooctene, obtained from the 1,3-butadiene and 1,5-cyclooctadiene through a metathesis reaction (see Fig. 1). Both cyclic and linear structures can be thus obtained [20]. The polymerization conditions determine the cis/trans ratio and thus the crystallinity degree. PCO behaves like an elastomer, and its application is often limited by the low melting temperature (i.e., slightly above ambient temperature). Above the melting temperature, crosslinked PCO behaves like a noncrystalline elastomer. Because of its peculiar properties, PCO is often applied in tyres production, in the rubber recycling process and in the asphalt as toughening and sound adsorbing agent. To improve the dimensional stability of the material, a crosslinking process is often required [19]. The chemical crosslinking with dicumylperoxide (DCP) [21, 22] allows to improve the dimensional stability of the material at elevated temperatures and to increase its mechanical response.

In literature it can be found that the investigation of the physical properties of PCO based nanocomposites has been limited to the optically and magnetically activated shape memory behavior [23]. For instance, Kunzelman et al. studied the shape memory behavior of PCO through chromogenic and fluorescent molecules [24], while Cuevas et al. studied the magneto-active shape memory properties of PCO composites filled with ferromagnetic particles [25]. Interestingly, no articles on the electroactive shape memory behavior of PCO nanocomposites can be found in the open literature.

In a recent work of our group [26], the electromechanical properties of PCO based nanocomposites, potentially applied as shape memory materials, were studied. CB, carbon nanofibers (NF) and exfoliated graphite nanoplatelets (xGnP) were melt compounded with a crosslinked PCO matrix at different amounts. In that article, it was highlighted how the introduction of CB and xGnP determined an enhancement of the elastic modulus of the material, without impairing its failure properties. Electrical resistivity measurements evidenced how the prepared composites could be interesting as electro-active materials for CB concentrations higher than 2 wt%. Taking into account these considerations and basing on the results of this preliminary work, the objective of the present paper is that to investigate the electro-activated shape memory behavior of a PCO based shape memory nanocomposite (SMN) device. Electrical resistivity measurements on bulk materials were performed, to detect the most promising compositions. The evolution of the surface temperature upon voltage application and the

Correspondence to: A. Dorigato; e-mail: andrea.dorigato@unitn.it
DOI 10.1002/pen.24590
Published online in Wiley Online Library (wileyonlinelibrary.com).

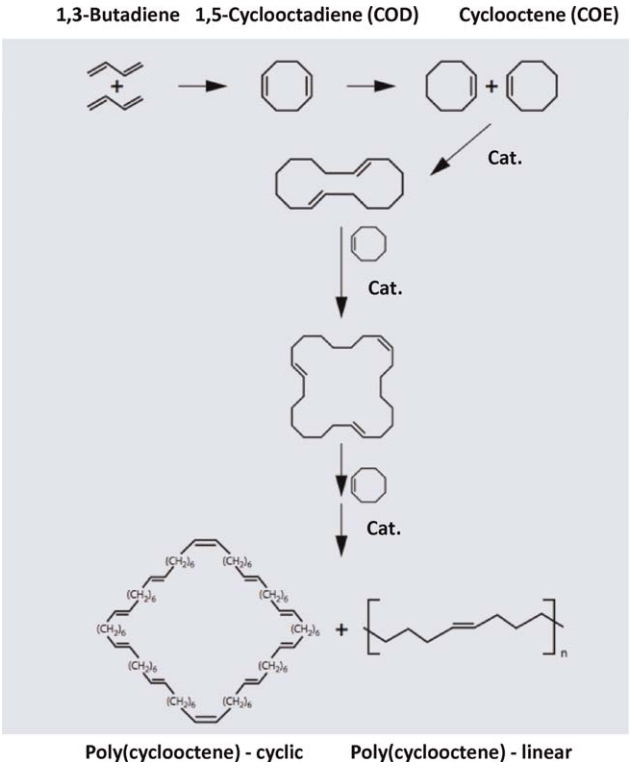

FIG. 1. Synthesis and chemical structure of PCO.

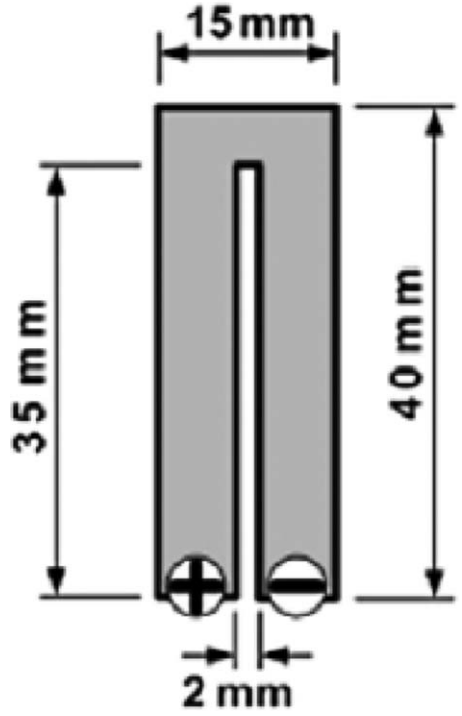

FIG. 2. Representation of the shape memory electro active device.

relative shape recovery degree of a shape memory device with optimized composition were then evaluated.

EXPERIMENTAL

Materials

Polymeric chips of a Vestenamer® 8012, provided by Degussa (Germany; mean molecular weight $M_w = 90{,}000$, $T_g = 65°C$, cis/trans ratio 20/80, density 0.91 g/cm^3) were used as PCO matrix. DCP powder, supplied by Sigma-Aldrich (molecular weight = 270.37, purity 98%) was utilized as chemical crosslinker. Ketjenblack EC600JD CB nanoparticles (mean particles size around 30 nm, density 1.95 g/cm^3, BET surface area 1,353 m^2/g) were provided by Akzo Nobel Chemicals Spa (Arese, Italy). M5-type Exfoliated Graphite Nanoplatelets (density = 2.05 g/cm^3, purity = 97 wt%, BET surface area 120 m^2/g, mean diameter 5 μm) were supplied by XG Science Inc. (East Lansing, USA). All the materials were used as received.

Preparation of the Samples

Bulk samples were prepared as reported in our preliminary work on these systems [26]. To obtain a good nanofiller dispersion without activating the crosslinking process, PCO granules and DCP were mixed in a Thermo Haake Reomix 600p compounder at 70°C for 5 min at a rotor speed of 5 min. The nanofiller was then introduced and compounded for other 5 min. The compounded materials were then hot pressed by using a Carver laboratory press at 180°C for 30 min, to obtain the complete crosslinking of the materials. Square sheet of neat PCO matrix and nanocomposites samples at different concentrations, with a mean thickness of 1 mm, were prepared. On the basis of the results of our preliminary work [26], a fixed DCP amount of 2 wt% and a total nanofiller loading of 4 wt% was used for all the samples. As reported in Table 1, in this article nanocomposite samples with CB and xGnP were considered. To evaluate possible synergistic effects, also nanocomposites with both nanofillers at two different relative CB/xGnP ratios were prepared.

TABLE 1. List of the prepared samples.

Sample	DCP content (wt%)	CB content (wt%)	xGnP content (wt%)
PCO_DCP_2_CB_4	2.0	4.0	—
PCO_DCP_2_xGnP_4	2.0	—	4.0
PCO_DCP_2_CB_75%_xGnP_25%	2.0	3.0	1.0
PCO_DCP_2_CB_90%_xGnP_10%	2.0	3.6	0.4

Experimental Techniques

Electrical Behavior of Bulk Materials. Electrical bulk resistance measurements in direct current mode on the nanocomposite samples were performed at room temperature through a 6 1/2-digit electrometer/high resistance system, provided by Keithley Instruments (Cleveland, OH), was used. A 2-point test configuration was chosen, and the surfaces of the samples in contact with the electrodes were painted with a silver coating to decrease the contact resistance. Rectangular samples (cross section of 5 × 1 mm^2, length of 100 mm) were tested, and at least five specimens were tested for each composition. As reported in our previous work on these systems [26], when the electrical resistance was lower than 10^5 Ω, measurements were performed under an applied voltage of 10 V, and the resistance values were measured after a time interval of 60 s. When the electrical

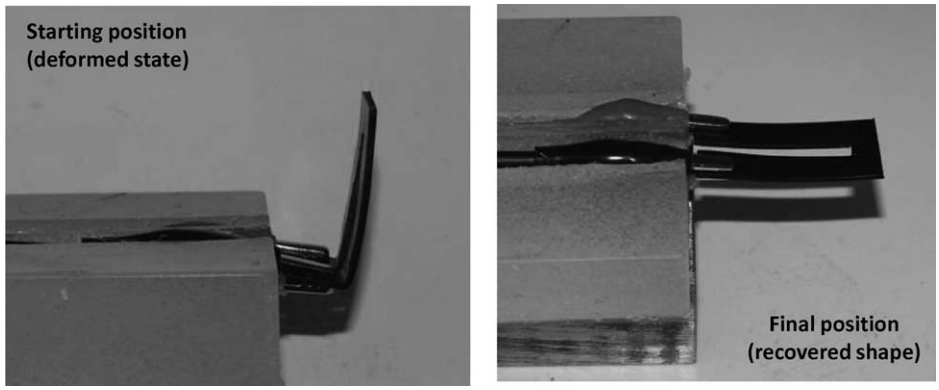

FIG. 3. Representation of the apparatus for the evaluation of the shape memory recovery degree.

resistance was between 10^5 and 10^{12} Ω, tests were performed under an applied voltage of 100 V. When the electrical resistance was higher than 10^{12} Ω, measurements with an applied voltage of 1,000 V were taken on square samples (length of 95 mm and thickness of 1 mm). In this case, coaxial electrodes were used to minimize the surface current flow.

Basing on the results of electrical resistivity measurements, surface temperature measurements on the PCO_DCP_2_CB_4 nanocomposite were performed, to evaluate the Joule heating effect produced by the current flowing through the samples upon voltage application. The same equipment and configuration used for electrical resistivity measurements was adopted, and various voltages ranging from 70 to 150 V were applied. The increase of the temperature produced by the electrical heating of the samples was monitored through an Optris® LaserSight infrared digital thermometer, acquiring an experimental point every 30 s.

Electroactive Shape Memory Behavior of a Nanocomposite Device. Basing on the results obtained on bulk materials, a shape memory device constituted by the PCO_DCP_2_CB_4 nanocomposite was prepared. A rectangular device cut from the prepared sheets having a length of 40 mm and a width of 15 mm was produced. As reported in Fig. 2, a cavity 35 mm long and 2 mm wide was created inside the sheet, and the electrodes were applied at the extremities of the device. The Joule heating effect produced by the current flow within the device was evaluated by a Fluke Ti9 infrared thermocamera. The evolution of the surface temperature in different zone of the device and the distribution of the heat flow were thus investigated.

The evaluation of the shape recovery degree of the device was performed by using the equipment reported in Fig. 3. The SM was fixed on a concrete block and connected to the electrodes. The device was heated through the application of a voltage of 100 V and the materials was deformed until the programming angular position (θ_f) was reached. After the complete cooling of the samples till room temperature, different voltage levels ranging from 70 to 150 V were applied. The shape recovery degree (D.R.) was measured considering the angular position reached by the material at the different times (θ_r). The shape recovery degree was determined as reported in *Eq. 1*:

$$\text{D.R.} = \left(\frac{\theta r - \theta f}{\theta i - \theta f}\right) \cdot 100 \quad (1)$$

where θ_i is the angular position of the undeformed material. To evaluate the repeatability of the shape memory effect, the same operation was repeated several times, and the recovery degree at different programming cycles was measured.

TABLE 2. Electrical bulk resistivity of the samples.

Sample	Electrical resistivity (Ω cm)
PCO_DCP_2_CB_4	$(1.4 \pm 0.1) \cdot 10^6$
PCO_DCP_2_xGnP_4	$(1.9 \pm 0.1) \cdot 10^{16}$
PCO_DCP_2_CB_75%_xGnP_25%	$(1.8 \pm 0.1) \cdot 10^6$
PCO_DCP_2_CB_90%_xGnP_10%	$(1.4 \pm 0.1) \cdot 10^6$

RESULTS AND DISCUSSION

Electrical Behavior of Bulk Materials

In Table 2, electrical bulk resistivity values of the nanocomposite samples with a filler amount of 4 wt% are reported. Considering that in the preliminary work [26] the electrical resistivity of the neat PCO matrix was measured as 1.1×10^{17} Ω cm, it is possible to observe how the introduction of xGnP is not able to determine a substantial reduction of the electrical resistivity. On the contrary, CB addition is able to promote a sensible resistivity drop up to 1.4×10^6 Ω cm. As reported in that article, this result can be probably ascribed to the good CB

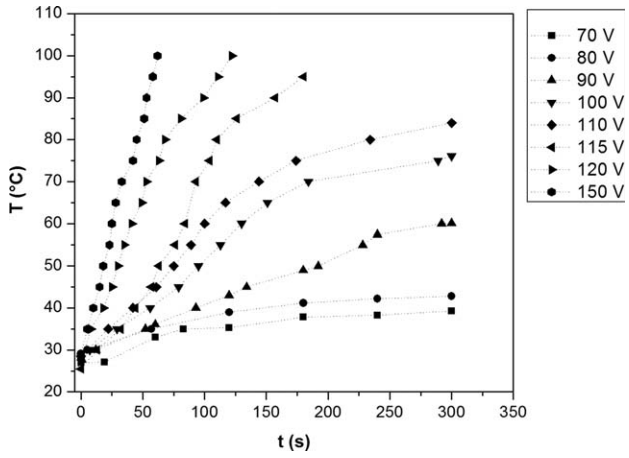

FIG. 4. Evolution of the surface temperatures at different voltages of the PCO_DCP_2_CB_4 sample.

 DOI 10.1002/pen

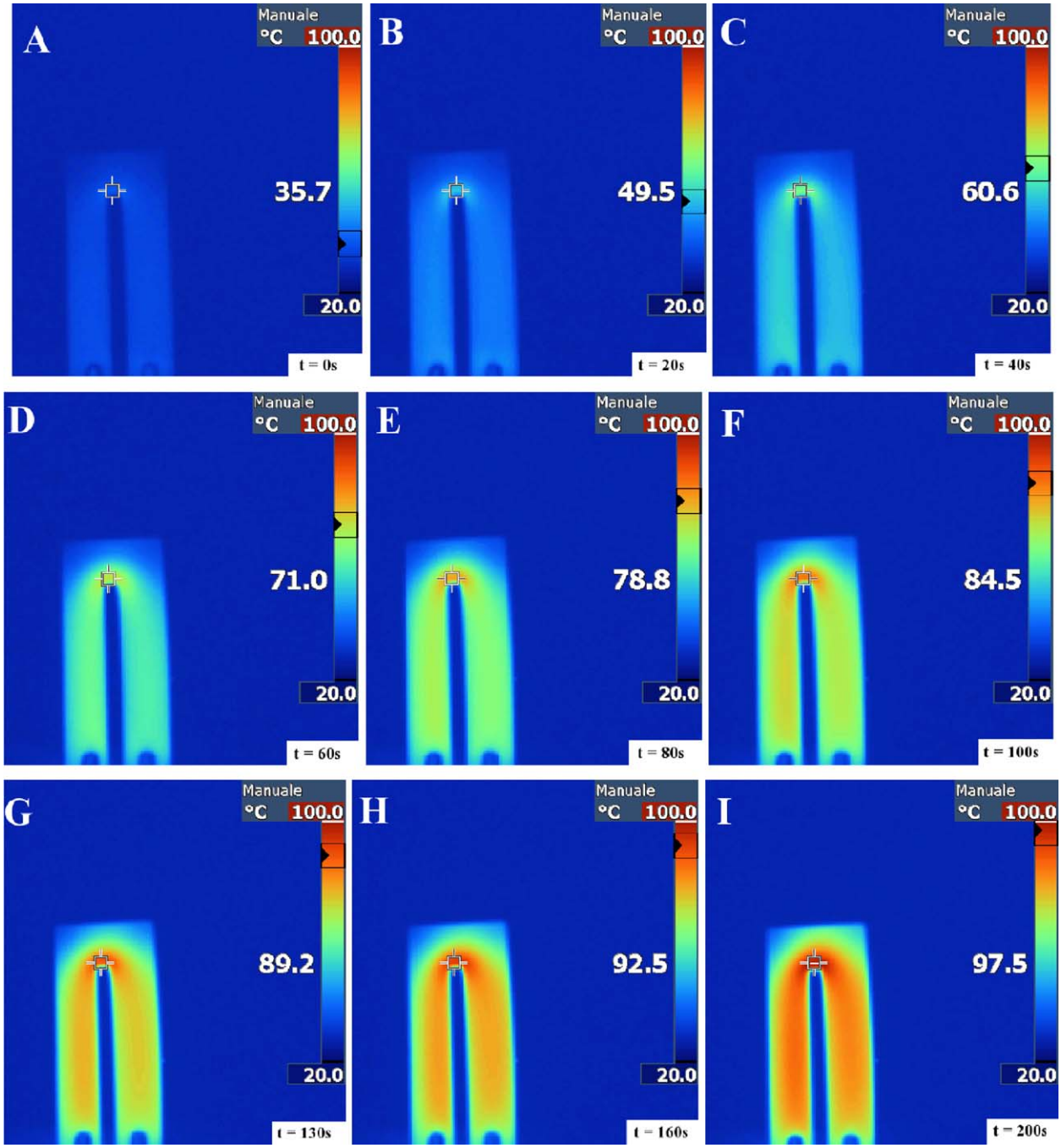

FIG. 5. Evolution of the surface temperatures of the prepared shape memory device (applied voltage 115 V). (a) Terminal zone and (b) lateral zone. [Color figure can be viewed at wileyonlinelibrary.com]

dispersion within the matrix and to the higher electrical conductivity of the CB with respect to the xGnP. To evaluate the possibility to obtain a further improvement of the electrical conductivity, also the electrical properties of nanocomposite samples with mixed composition were measured. As reported in Table 2, the addition of both nanofillers does not promote a further improvement of the electrical properties of the samples. This result is in contrast with some articles in literature [12, 27], in which the synergistic effect observed in nanocomposites with mixed composition was explained through the formation of a percolative network within the matrix. Moreover, also in our previous article on PLA based nanocomposites it was reported how the combination of vapor grown carbon fibers (VGCF) and exfoliated graphite nanoplatelets (xGnP) fillers promoted a further decrease of surface resistivity with respect to the corresponding binary systems [28]. Similar conclusions were drawn also in our previous work on epoxy based nanocomposite systems, in which the electrical resistivity of the epoxy matrix was dramatically reduced by the simultaneous addition of CB and carbon NF at a total nanofiller amount of 2 wt% [5]. In both cases, these result were ascribed to the formation of a three dimensional conductive network within the matrix. In this case,

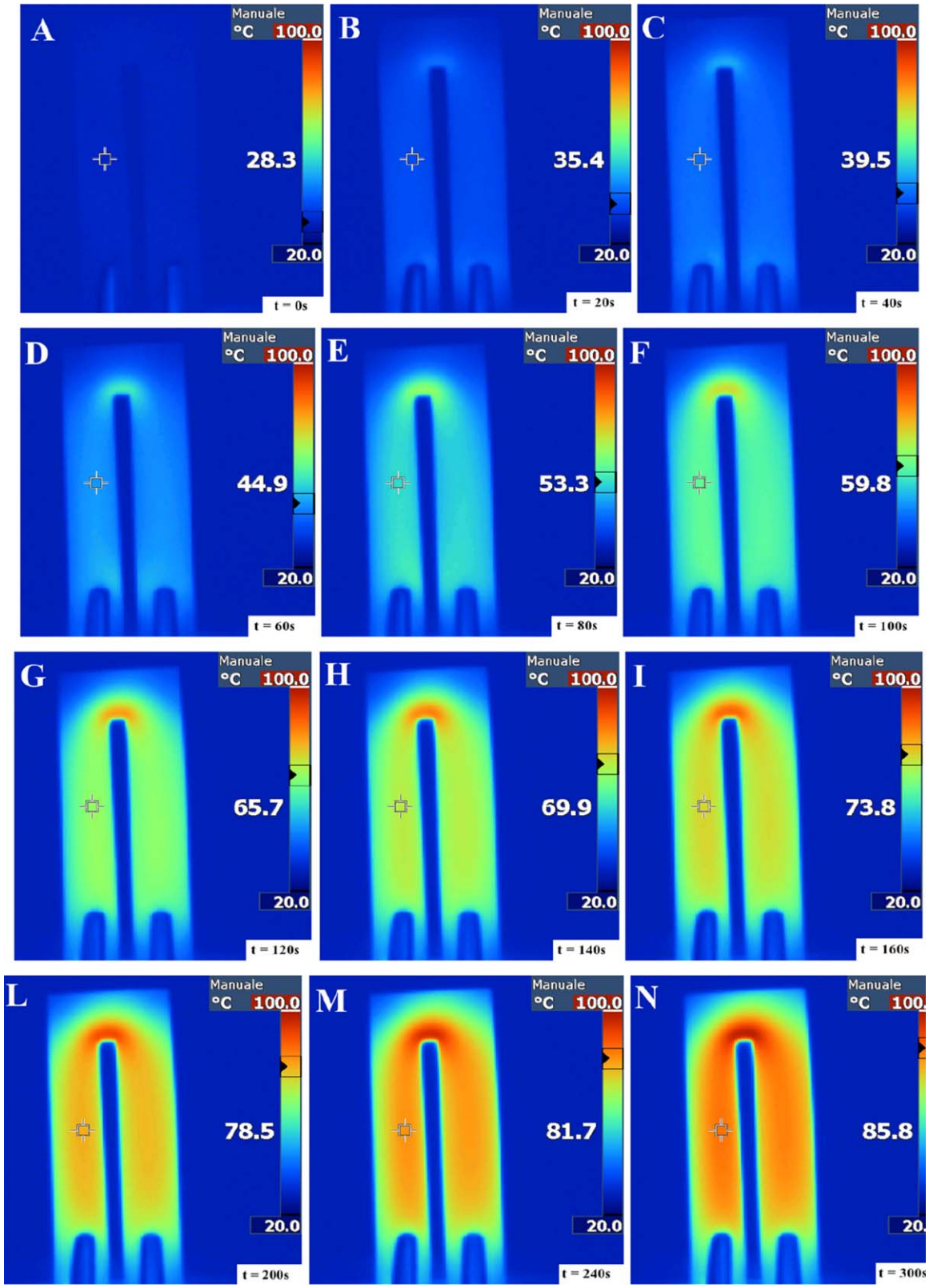

FIG. 5. (Continued).

it is possible that the dispersion of the filler within the matrix did not allow the formation of a percolative network able to support the current flow within the material. Therefore, only PCO_DCP_2_CB_4 nanocomposite sample was considered for the preparation of the electro-active shape memory device.

Considering that the electro-active behavior of shape memory materials is based on their heating capability upon voltage application, surface temperature measurements were performed by varying the potential applied to the material. In Fig. 4, the evolution of the surface temperatures at different voltages on

 DOI 10.1002/pen

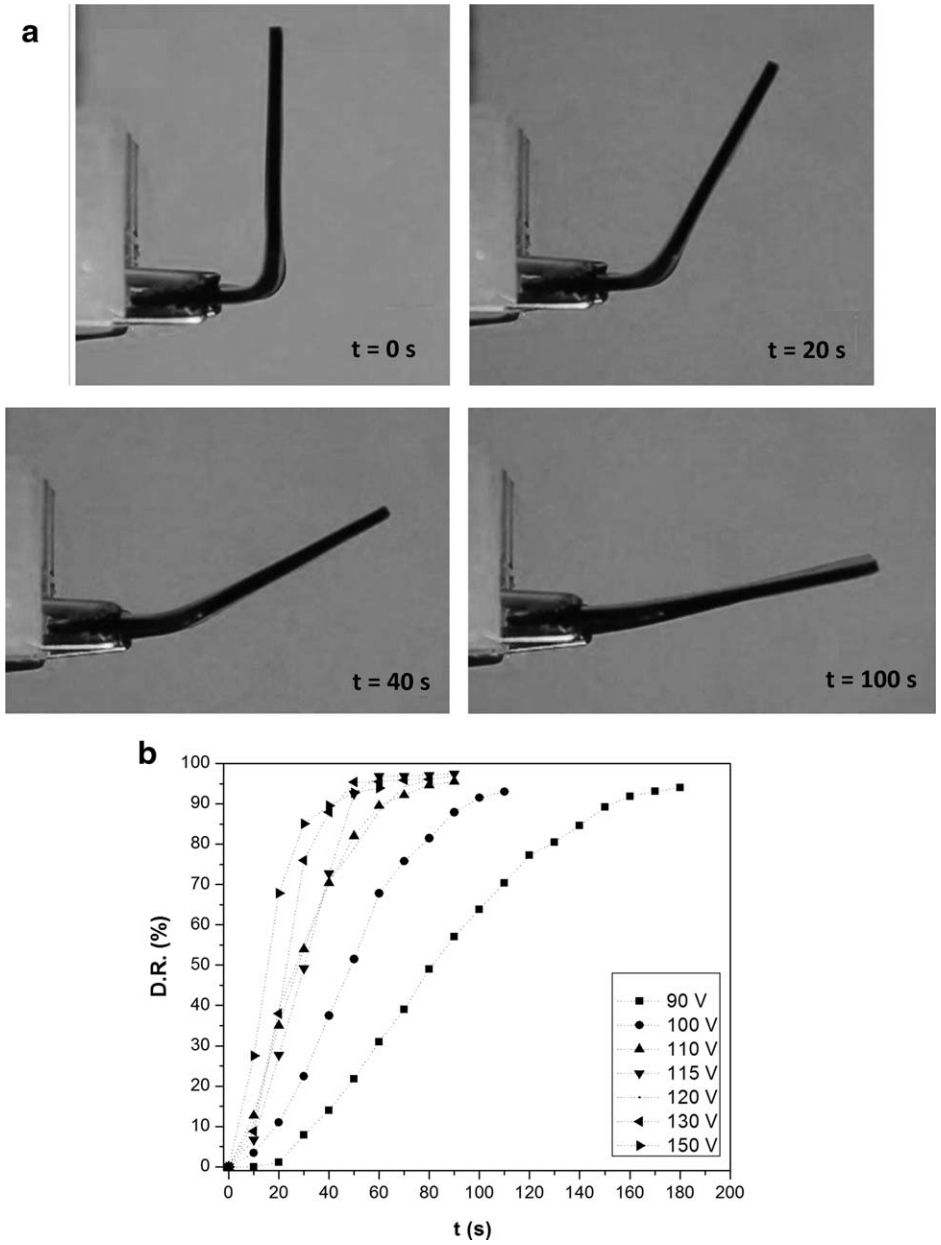

FIG. 6. Shape memory behavior of the electroactive shape memory device; (a) shape recovery at different times (applied voltage 115 V) and (b) shape recovery degree at different voltage levels.

the PCO_DCP_2_CB_4 sample was reported. Considering that the melting temperature (T_m) of the PCO_DCP_2_CB_4 nanocomposite measured through DSC tests was 47.9°C [26], it is possible to conclude that applying voltage levels below 90 V is not sufficient to reach the transition temperature of the material. At 90 V, T_m can be reached after a time interval of more than 3 min. This time is probably too long for the industrial application of this materials. However, applying a voltage of 150 V a too rapid temperature increase can be observed. In these conditions, the control of the temperature within the material is practically impossible, and thermal degradation of the device could occur. It can be therefore concluded that the optimal voltage range for this device is between 100 and 120 V.

Electroactive Shape Memory Behavior of a Nanocomposite Device

Considering that the electroactive behavior of a shape memory materials is based on their heating capability upon voltage application, the optimal composition of the shape memory device was selected on the basis of the electrical conductivity results of bulk materials. Therefore, a shape memory device based on the PCO_DCP_2_CB_4 nanocomposite material was prepared, and its thermoelectrical behavior was investigated. In Fig. 5a and b, the evolution of the surface temperatures of the prepared shape memory device at an applied voltage 115 V in the terminal and in the lateral zones is shown. It is interesting to note how the distribution of the temperature within the device is not homogeneous, and that the maximum temperature is reached in the terminal region of the device. It is probable that in this

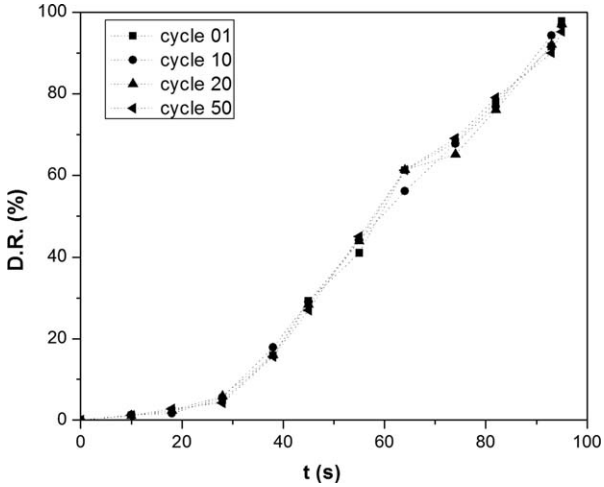

FIG. 7. Shape memory recovery degree of the prepared device at different programming cycles (applied voltage 115 V).

point a concentration of the current flow due to geometrical reasons occurred, and the surface temperature is thus increased. For this reason, similar voltage application times systematically induce higher temperature in the terminal zone (Fig. 5a) compared with the lateral section (Fig. 5b) of the device. However, it is important to underline that after 60 s all the zones of the device reach a temperature higher than that required for the activation of the shape memory effect (i.e., the T_m of the material).

At this point, the shape memory behavior of the electroactive SM device was evaluated. In Fig. 6a, shape recovery at different times with an applied voltage of 115 V is shown, while in Fig. 6b shape D.R. at different voltage levels is reported. It is interesting to note that applying 115 V the material is able to reach a D.R. of 50% in 30 s, while the original shape is recovered in $<$100 s. It is also clear that the prepared device shows an almost complete recovery of the original shape over the whole range of considered voltages. As it could be predicted, the speed of the recovery is proportional to the voltage. The highest shape recovery degree can be obtained in a voltage interval between 110 and 150 V.

It is also important to evaluate the durability of the shape memory effect at repeated programming cycles. At this scope, D.R. at an applied voltage of 115 V was evaluated after 50 thermal cycles. As reported in Fig. 7, it can be concluded that D.R. kinetics are not influenced by the number of cycles, and the device is able to reach an almost complete recovery of the original shape even after 50 programming cycles. Considering that in some articles in literature the shape memory recovery was shown to sensibly decrease after repeated thermal cycles [8, 29], the results obtained in this work confirmed the thermal stability of the PCO matrix and of the prepared device.

CONCLUSIONS

In this work, the electroactive shape memory behavior of a PCO based SMN device was investigated. Nanocomposite samples filled with CB and xGnP at a constant filler amount of 4 wt% and crosslinked with a DCP content of 2 wt% were prepared through melt compounding process and thermoelectrically characterized. An interesting decrease of the electrical resistivity up to 10^6 Ω·cm, coupled with a noticeable heating capability through Joule effect for voltage levels higher than 100 V, could be obtained with a CB amount of 4 wt%. The electrical characterization of an electroactive shape memory device based on this composition highlighted how an almost complete shape recovery could be obtained shape after 100 s applying voltage levels of 90 V. Interestingly, the shape memory behavior could be maintained even after several programming cycles.

ACKNOWLEDGMENT

Mr. Simone Brazzo is gratefully acknowledged for his support to the experimental work.

REFERENCES

1. Z.J. Fan, C. Zheng, T. Wei, Y.C. Zhang, and G.L. Luo, *Polym. Eng. Sci*., **49**, 2041 (2009).
2. J. Li, P.S. Wong, and J.K. Kim, *Mater. Sci. Eng. A Struct. Mater. Properties Microstruct. Proc*., **483–484**, 660 (2008).
3. J. Sumfleth, S.T. Buschhorn, and K. Schulte, *J. Mater. Sci*., **46**, 659 (2010).
4. M. Traina, A. Pegoretti, and A. Penati, *J. Appl. Polym. Sci*., **106**, 2065 (2007).
5. D. Pedrazzoli, A. Dorigato, and A. Pegoretti, *J. Nanosci. Nanotechnol*., **12**, 4093 (2012).
6. D. Pedrazzoli, A. Dorigato, and A. Pegoretti, *Compos. A*, **43**, 1285 (2012).
7. R. Bogue, *Assembly Autom*., **29**, 214 (2009).
8. A. Lendlein, and S. Kelch, *Angew. Chem. Int. Ed*., **41**, 2034 (2002).
9. J.W. Cho, J.W. Kim, Y.C. Jung, and N.S. Goo, *Macromol. Rapid Commun*., **26**, 412 (2005).
10. I.H. Paik, N.S. Goo, Y.C. Jung, and J.W. Cho, *Smart Mater. Struct*., **15**, 1476 (2006).
11. H. Koerner, G. Price, N. Pearce, M. Alexander, and R.A. Vaia, *Nat. Mater*., **3**, 115 (2004).
12. J.S. Leng, H.B. Lv, Y.J. Liu, and S.Y. Du, *Appl. Phys. Lett*., **91**, (2007).
13. A.M. Schmidt, *Macromol. Rapid Commun*., **27**, 1168 (2006).
14. M. Drubetski, A. Siegmann, and M. Narkis, *J. Mater. Sci*., **42**, 1 (2007).
15. H.Z. Geng, R. Rosen, B. Zheng, H. Shimoda, L. Fleming, J. Liu, and O. Zhou, *Adv. Mater*., **14**, 1387 (2002).
16. Y. Lin, B. Zhou, K.A.S. Fernando, P. Liu, L.F. Allard, and Y.P. Sun, *Macromolecules*, **36**, 7199 (2003).
17. C. Velasco-Santos, A. Martinez-Hernandez, F.T. Fisher, R. Ruoff, and V.M. Castano, *Chem. Mater*., **15**, 4470 (2003).
18. A. Dorigato, G. Giusti, F. Bondioli, and A. Pegoretti, *Express Polym. Lett*., **7**, 673 (2013).
19. C. Liu, S.B. Chun, P.T. Mather, L. Zheng, E.H. Haley, and E.B. Coughlin, *Macromolecules*, **35**, 9868 (2002).
20. J.C. Mol, *J. Mol. Catal. A: Chem*., **213**, 39 (2004).
21. M. Baba, J.L. Gardette, and J. Lacoste, *Polym. Degrad. Stab*., **63**, 121
22. M. Baba, S. George, J.L. Gardette, and J. Lacoste, *Polym. Int*., **52**, 863 (2003).
23. J. Leng, X. Lan, Y. Liu, and S. Du, *Prog. Mater. Sci*., **56**, 1077 (2011).
24. J. Kunzelman, T. Chung, P.T. Mather, and C. Weder, *J. Mater. Chem*., **18**, 1082 (2008).

 DOI 10.1002/pen

25. M. Cuevas, J. Alonso, L. German, M. Iturrondobeitia, J.M. Laza, J.L. Vilas, and L.M. Leon, *Smart Mater. Struct.*, **18, 1**, (2009).
26. A. Dorigato and A. Pegoretti, *Polym. Eng. Sci.*, **57**, 537 (2016).
27. J. Sumfleth, X.C. Adroher, and K. Schulte, *J. Mater. Sci.*, **44**, 3241 (2009).
28. M. Tait, A. Pegoretti, A. Dorigato, and K. Kaladzidou, *Carbon*, **49**, 4280 (2011).
29. M. Behl and A. Lendlein, *Mater. Today*, **10**, 20 (2007).